Luminescent properties of $Y_3Al_5O_{12}$ nanograined ceramics and single crystals

Yu.Zorenko[1,2], *T.Voznyak*[2], *V.Gorbenko*[2], *A.Doroshenko*[3], *A.Tolmachev*[3], *R.Yavetskiy*[3], *I.Petrusha*[4], *V.Turkevich*[4]

[1]Institute of Physics of Kazimierz Wielki University of Bydgoszcz, 11 Weyssenhoffa Sq., 85-072 Bydgoszcz, Poland
[2]Electronics Department of I.Franko National University of Lviv, 107 Gen. Tarnavsky Str., 79017 Lviv, Ukraine
[3]Institute for Single Crystals, STC "Institute for Single Crystals", National Academy of Sciences of Ukraine, 60 Lenin Ave., 61001 Kharkiv, Ukraine
[4]V.Bakul Institute for Superhard Materials, National Academy of Sciences of Ukraine, 2 Avtozavodskaya Str., 04074 Kyiv, Ukraine

Received January 12, 2012

The optical transmittance in the visible wavelength range, thermally stimulated luminescence and time-resolved luminescence under excitation by synchrotron radiation in the exciton range of $Y_3Al_5O_{12}$ host were studied to characterize $Y_3Al_5O_{12}$ nanograined ceramics in comparison to single crystals of the same composition. The behavior of nanograined ceramics is situated close to the properties of single crystals with large content of Y_{Al} antisite defects. The observed differences in the optical and luminescent properties were interpreted as a consequence of high defectivity level of nanograined ceramics arising from its non-equilibrium character and high concentration of grain boundaries.

Проведено сравнительное исследование оптического пропускания, термостимулированной люминесценции и фотолюминесценции с временным разрешением при возбуждении синхротронным излучением в области фундаментального поглощения нанозеренной керамики $Y_3Al_5O_{12}$ и монокристаллов аналогичного состава. Поведение нанозеренной керамики близко к таковому для монокристаллов с большой концентрацией антиструктурных дефектов Y_{Al}. Наблюдаемые различия в оптических и люминесцентных свойствах кристаллов и нанокерамики $Y_3Al_5O_{12}$ обусловлены более высокой степенью дефектности нанозеренной керамики, связанной с неравновесным характером ее получения и высокой концентрацией межзеренных границ.

1. Introduction

Nanograined ceramics (NC) with a typical grain size less than 100 nm based on $Y_3Al_5O_{12}$ (YAG) represents a new type of optical materials perspective for application in photonics, laser and scintillation techniques. The main distinctive feature on nanoceramics is extremely high concentration of atoms within grain boundaries, normally from 10 to 50 %. As a result, optical and electronic properties of nanoceramics are substantially different in comparison with bulk materials. For instance, nanograined Al_2O_3 shows new luminescence band originated from surface F_S^+-centers; has faster luminescence decay and higher luminescence yield compared to corresponding single crystals [1]. Differences in optical properties of the nano- and single-crystalline form of other garnet matrix $Y_3Fe_5O_{12}$ were observed in [2]. Studies of luminescent properties of YAG nanoceramics are limited only by activated materials [3–

6]. Luminescent properties of nominally undoped YAG nanoceramics are insufficiently presented in modern literature. Recently in works [7, 8] we have compared the luminescent properties of YAG:Ce single crystals (SC), single crystalline films (SCF), nanopowders (NP) and transparent microceramic (MC) under excitation by synchrotron radiation (SR) in the VUV range. We showed [7, 8] that the differences in the spectral-kinetic characteristics of the Ce^{3+} luminescence in YAG:Ce phosphors are caused by the significant differences in preparation methods; namely the concentration of antisite defects (AD) and oxygen vacancies as main types of defects in garnet compounds. These types of defects can play the role as emission and trapping centers and strongly contributed to the energy transfer processes from YAG host to Ce^{3+} emission centers. In this work we continue our research of the luminescent properties of the different crystalline forms of YAG. The aim of this work is to compare the intrinsic luminescence of YAG NC and SC under excitation by synchrotron radiation in the exciton range of YAG host. YAG is not only excellent laser and scintillation material, but also an attractive model object for investigation of optical properties in nanocrystalline forms due to well-known optical properties for the bulk SC form [9,10] .

2. Experimental

Custom-made $Y_3Al_5O_{12}$ low-agglomerated nanopowders were produced by reverse strike co-precipitation method with addition of sulfate ions as a dispersant. Sulfate ions adsorbed onto the particle surface form double electric layer thus increasing interparticle repulsion forces and improving powder dispersity. The single-phase YAG powders were consolidated under the thermobaric static conditions at a toroid-type high-pressure apparatus. The consolidation was carried out under 7.7 GPa pressure in the 25–550°C temperature range [11, 12]. The YAG SC were crystallized from the melt at 1970°C by the Czochralski method. Significant difference in the preparation conditions of YAG SC and NC (fabrication temperature, atmosphere, pressure etc.) is strongly reflected on the concentration of Y_{Al} AD (Y cations in the positions of Al cations) and oxygen vacancies and related emission and trapping centers [7, 8, 13–15]. The total transmittance of YAG SC and NC samples in the 250–1100 nm wavelength range was studied on a Perkin-Elmer "Lambda-35" spectrophotometer using integrating sphere. The TSL glow curves of YAG SC and NC were recorded using a home-made setup equipped with a FEU-79 PMT at a heating rate of 5 K/min. The samples were irradiated with X-quanta (RUP150/300-10-1 X-ray unit, Cu anode; U = 160 kV, I = 9 mA) at room temperature. Comparative analysis of the time-resolved intrinsic luminescence of YAG and YAG:Ce NC and SC has been performed under excitation by pulsed (0.127 ns) SR at the Superlumi experimental station (HASYLAB at DESY) with an energy of 3.7–25 eV. The emission and excitation spectra were measured with monochromators ARC and PMT Hamamatsu R6358P, both in the integral regime and in the 1.2–12 and 150–200 ns time intervals (fast and slow components, respectively) in the limits of SR pulse with a repetition time of 200 ns. The decay kinetics of luminescence was measured in the 0–200 ns time range at 10 K. The excitation spectra were corrected for the spectral dependence and intensity of the excitation energy; the emission spectra were not corrected.

3. Results and discussion

High-pressure sintering is a powerful tool to produce dense nanograined ceramics due to activation of the consolidation process via active movement of particles as a whole, destruction of agglomerates and closing of large pores. YAG translucent nanograined ceramics with a density of 99±2 % has been produced under P = 7.7 GPa and the temperature of about 0.2 of YAG melting point. The ceramics has average grain size of 20–40 nm, comparable to that of the initial nanopowders (38.5 nm). Thickness of grain boundaries of YAG nanoceramics ranges from 1 to 2 nm. The nanoceramics characterize by negligible residual porosity with a typical pore size in the nanoscale range (~10 nm) [11, 12].

Fig. 1 shows the total transmittance spectrum of roughly-polished YAG nanograined ceramics. The transmittance of 63 % at λ = 1064 nm achieves 75 % of theoretical value (84 % in the visible wavelength range). As known, residual porosity is a main factor governing the transparency of ceramics due to large difference in refractive indexes between the ceramics and gas-filled pores. The maximal scattering occurs when the pore size is equal to the wavelength of incident light. In our case pores are too small (10 nm) to produce sig-

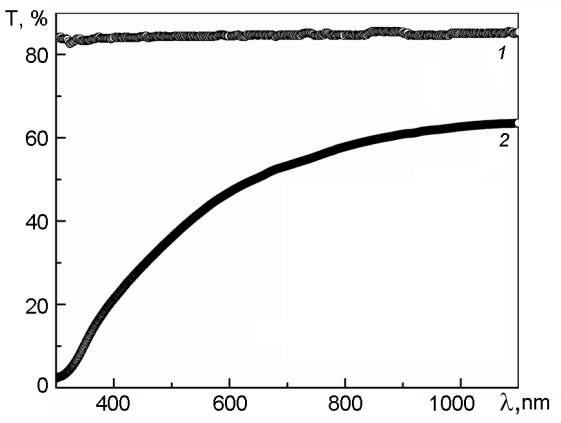

Fig. 1. Total transmittance of 1 mm thick $Y_3Al_5O_{12}$ single crystal (*1*) and nanograined ceramics (*2*) sintered for 60 s at a pressure of ~7.7 GPa and temperature of 350°C.

nificant scattering [12]. This means that another mechanism of light scattering exist in our samples, namely light absorption by micro-defects or additional scattering of light by rough surfaces of ceramics, since the size of structural units forming ceramics (grains, pores and grain boundaries) is much smaller than visible light.

Taking into account extremely high extension of grain boundaries and increased concentration of point defects in nanograined ceramics, one can assume that defect structure of ceramics could be revealed in luminescent recombination processes, such as thermally stimulated luminescence (TSL). Fig. 2 shows TSL glow curves of YAG SC and NC obtained at heating rate of 5 K/min after irradiation with X-ray quanta (9000 R dose). The deconvolution of experimental plots into elementary peaks was done by GlowFit software assuming first-order kinetics [16]. The TSL curves of YAG SC and NC are non-elementary and consist of groups of peaks in the 300–525 K temperature range. TSL of single crystal contains several peaks at T = 330, 370, 400 and 500 K, idicating the presence of four traps of charge carriers (Fig. 2, a). The activation energy of main TSL peak at T = 500 K is 1.55 eV. The glow curve of nanoceramics demonstrates significant distinctions as compared to single crystals and presents superposition of number of peaks quasi-continuously distributed in the T = 300–525 K range. Although at least six peaks can be revealed in the TSL glow-curve, we failed to correctly estimate their energetical parameters because the peaks are strongly overlapped (Fig. 2, b). The light sum storaged by nanoceramics is

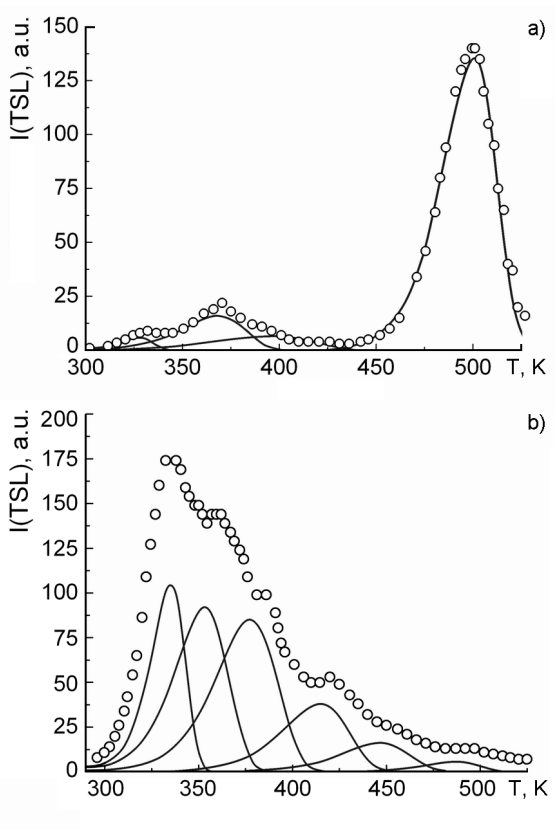

Fig. 2. TSL glow curves of $Y_3Al_5O_{12}$ single crystal (a) and $Y_3Al_5O_{12}$ nanograined ceramics (b) irradiated with X-ray quanta (9000 R dose). The open circles denote experimental points, the solid lines — fitting by first order kinetics.

2.5 times higher than that of single crystals, specifying the higher concentration of point defects trapped the charge carriers.

As known, energy of X-ray quanta (E = 30 keV) is insufficient to create stable radiation defect in complex oxides by impact mechanism, because relatively high threshold displacement energy. Formation of displacement defects in YAG anionic sublattice requires energy of 40 eV [17]. For this reason observed TSL is most likely connected with "recharging" of genetic (intrinsic or growth) defects or impurity ions. Strictly speaking, the presence of thermally stimulated luminescence allows only make conclusions about number of defects and their activation energy (location of levels of defects in band gap), not on their nature. Assuming identical radiative recombination mechanisms for both YAG SC and NC single crystals and nanograined ceramics, one can conclude the higher deficiency of nanoceramics. The shape of TSL curve of nanoceramics demonstrates similarity with oxide glasses having quasy-continuous distribution of

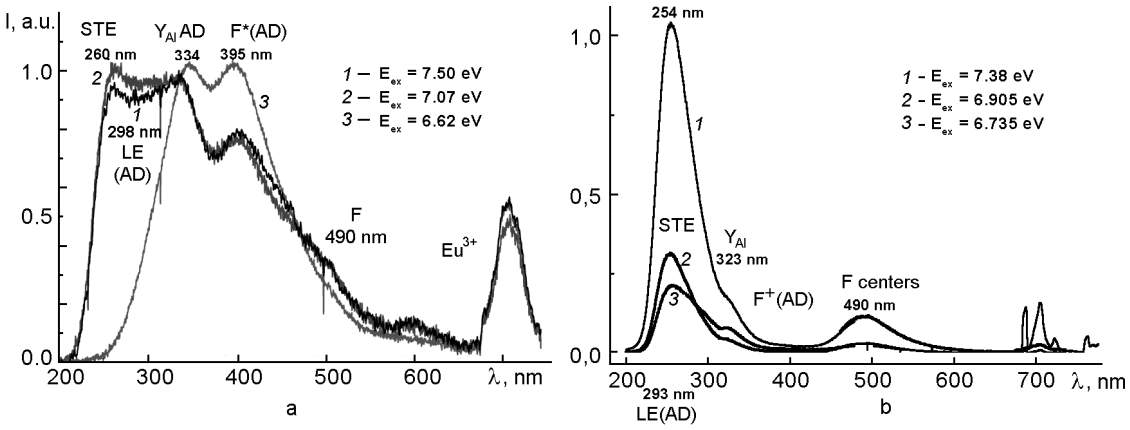

Fig. 3. Luminescence spectra of YAG NC (a) and SC (b) at 10 K under excitation by SR with energies indicated in legend of figures, in the exciton range of YAG host.

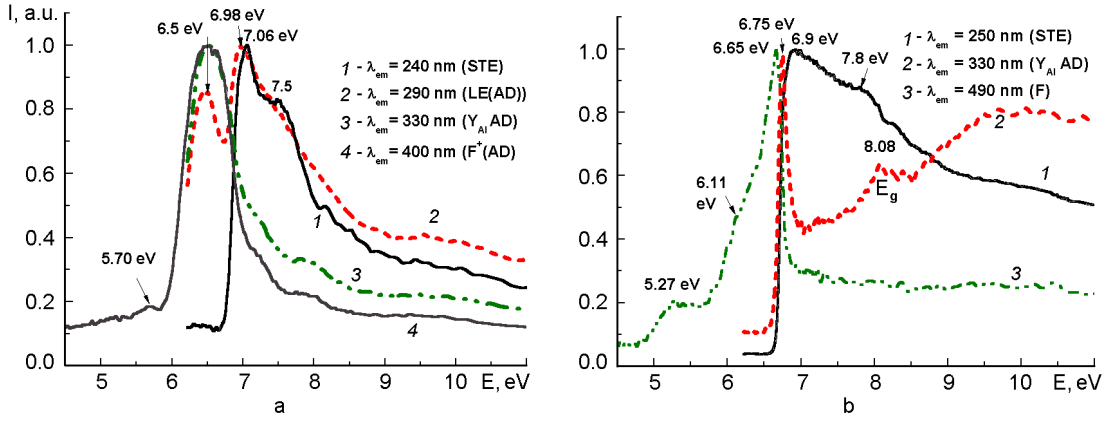

Fig. 4. Excitation spectra of the different emission centers in YAG NC (a) and SC (b) at 10 K.

traps. Numerous grain boundaries, surface states and microstrains presented in nanoceramics leads to redistribution of existing and to creation of new traps not typical for single crystals.

The luminescence spectra of YAG NC (a) and SC (b) at 8 K under excitation by SR with different energies in the YAG exciton range are shown in Fig. 3. The normalized emission spectra of YAG NC (Fig. 3a) consist of the set of broad bands in the UV and blue ranges peaked at 260, 298, 334, 395 and 490 nm. By analogy with the well-known structure of the intrinsic luminescence of YAG SC (Fig. 3b) [13–15], the mentioned emission bands of YAG NC are caused by the radiation decay of a self-trapped excitons (STE) and excitons, localized around Y_{Al} AD (LE(AD) centers); the recombination emission of Y_{Al} AD; the luminescence of F^+ centers (oxygen vacancy with one trapped electron), localized around Y_{Al} AD and the emission of F centers (oxygen vacancy with two trapped electron), respectively. The luminescence bands of YAG NC in the orange-red range are caused by Eu^{3+} trace impurity (Fig. 3a).

The intensity of the luminescence of STE and Y_{Al} AD related centers is at least by one order of magnitude lower in YAG NC (Fig. 3a) than that in the SC counterpart (Fig. 3a). Specifically, at 8 K the STE luminescence in the 254 nm band is dominating in the spectra of YAG SC (Fig. 3a) whereas for YAG NC the intensity of STE emission is comparable with the intensity of AD-related bands and F^+ centers (Fig. 3b). This result shows that Y_{Al} AD and charged oxygen vacancies strongly contribute to the total output of the intrinsic luminescence of YAG NC. The concentration of these intrinsic defects is very high at the boundaries of NC grains and strongly decreases in the main volume of YAG NC [7, 8].

The excitation spectra of the different intrinsic emission centers in YAG NC (a)

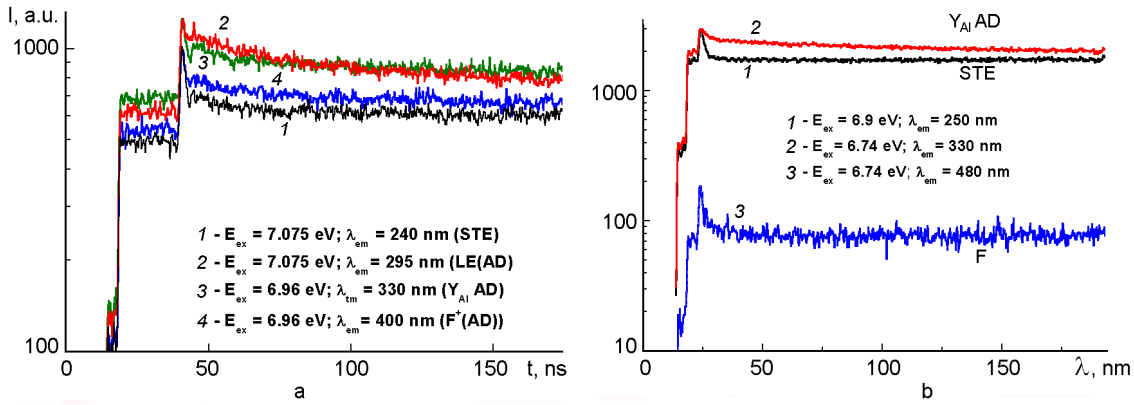

Fig. 5. Decay kinetics of different emission centers in YAG NC (a) and SC (b) at 10 K under excitation by SR with energies, indicated in figures.

and SC (b) at 10 K are shown in Fig. 4. Apart from the generally the same structure of excitation bands, we find some important differences in the excitation spectrum of YAG NC with respect to the excitation spectra of the similar centers in YAG SC. Namely, positions of the excitation bands of STE emission in YAG NC at 7.06 and 7.5 eV differ from the positions of the same bands at 6.9 and 7.8 eV in the excitation spectrum of the SC counterpart. Such a significant low-energy shift (~0.16 eV) of the main excitation band of the STE emission in YAG SC with respect to the excitation spectrum of YAG NC reflects the dominant contribution of Y_{Al} AD to their luminescent properties. As oppose to YAG SC, position of the main excitation band of the STE luminescence of YAG NC (with lower than in SC concentration of AD in the main volume [7]) is closer to position of the STE bands in YAG single crystalline films at 7.17 eV [14, 15], where the AD are completely absent.

The main band in the excitation spectrum of the Y_{Al} AD luminescence at 334 nm in YAG NC (Fig. 4a, curve *3*) is significantly broader and strongly low-energy shifted to 6.6 eV with respect to position of the narrow peak at 6.75 eV for AD emission in YAG SC (Fig. 4b, curve *2*). This result reflects strong involving other defect centers, namely, the oxygen vacancies, in the formation of energy structure of Y_{Al} centers in YAG NC. The last conclusion is also supported by very close structure of the excitation spectra of the emission of Y_{Al} AD and F^+(AD) center in YAG NC in the exciton range (Fig. 4a, curves *3* and *4*, respectively). The excitation spectrum of the F^+ (AD) center luminescence in YAG NC (Fig. 4a, curve *4*) is also notably broader in the exciton range and is shifted to 6.5 eV in comparison with the excitation spectrum of the *F*-center luminescence in YAG SC (Fig. 4b, curve *3*) with main maximum at 6.65 eV and bumps at 6.11 and 5.27 eV. Therefore, the strong coupling of the AD and oxygen vacancy-related centers is expected in YAG NC, mainly at the boundaries of grains [7, 8].

The decay kinetics of the luminescence of STE and different defects centers in YAG NC and SC is shown in Fig. 5. All of the decay curves present the typical superposition of fast (in range of few ns) and slow (in the range of hundred ns-μs) emission components, presumable corresponding to the singlet-singlet and triplet-singlet radiation transitions [13, 14]. Such a type of the decay kinetics is characteristic for the radiation decay of STE or excitons localized around all intrinsic defects as well as for the luminescence of excitons bound with the mentioned defects of YAG host [7, 8, 13, 14]. From comparison of the corresponding decay curves in Fig. 5, we find that the decay kinetics of the same centers is faster in YAG NC (Fig. 5a) than in YAG SC (Fig. 5b). Most probably that such differences in the shape of the decay curves for the same centers reflect the difference in the relative concentrations of Y_{Al} AD, F^+, *F* centers and their aggregates in the samples under study.

4. Conclusions

It has been shown that YAG nanograined ceramics has much more defect structure compared to corresponding single crystals resulting in higher intensity of thermally stimulated luminescence. The analysis of the luminescent properties of YAG nanoceramics in comparison with single crystal

analogues allows us to conclude that the behavior of NC is situated clothe to the properties of SC with large content of Y_{Al} antisite defects. The complex intrinsic UV luminescence of YAG NC in 200–500 nm range as well as that of YAG SC is caused by the radiation decay of self-trapped excitons and exciton, localized around Y_{Al} antisite defects; the recombination emission of Y_{Al} AD themselves; the luminescence of F^+ centers, localized around Y_{Al} AD as well as the intrinsic emission of F centers. Y_{Al} AD and charged oxygen vacancies significantly contribute to the total output of the intrinsic luminescence of YAG NC. The relative intensity of F^+ centers is significantly higher in YAG NC than that for SC counterpart. This presupposes the strong coupling of the AD and oxygen vacancy-related centers in YAG NC, mainly at the boundaries of grains. The position of the main excitation band of the STE luminescence in YAG NC at 7.07 eV is significantly (~0.16 eV) high-energy shifted with respect to the same band in the YAG SC counterpart indicating strong decrease the concentration of Y_{Al} AD in the main volume of YAG NC with respect to the SC analogues.

Acknowledgments. The investigation with synchrotron radiation at the Superlumi station was performed in the framework of I-20110085 EC project. Authors also are grateful for the support from Target Complex Program of Fundamental Research of NAS of Ukraine "Fundamental problems of Nanostructured Systems, Nanomaterials and Nanotechnologies", Project No.78/10-H and Ministry of Education and Science of Ukraine (Project No. SL-126 F).

References

1. V.S.Kortov, A.E.Ermakov, A.F.Zatsepin et al., *Phys. Solid State*, **50**, 957 (2008).
2. A.A.Makhnev, B.A.Gizhevskii, L.V.Nomerovannaya, *J. Exp. Theor. Phys. Lett.*, **91**, 79 (2010).
3. D.Hreniak, W.Strek, P.Gluchowski et al., *J. Alloys Compd.*, **451**, 549 (2008).
4. D.Hreniak, M.Bettinelli, A.Speghini et al., *J. Nanosci. Nanotechnol.*, **9**, 6315 (2009).
5. W.Zhao, D.Hreniak, G.Boulon et al., *Radiat. Meas.*, **45**, 304 (2010).
6. V.Pankratov, L.Shirmane, T.Chudoba et al., *Radiat. Meas.*, **45**, 392 (2010).
7. Yu.Zorenko, T.Voznyak, V.Gorbenko et al., *J. Lumin.*, **131**, 17 (2011).
8. Yu.Zorenko, E.Zych, A.Voloshinovskii, *Opt. Mater.*, **31**, 1845 (2009).
9. J.Lu, K.Ueda, H.Yagi et al., *J. Alloys Compd.*, **341**, 220 (2002).
10. I.Kamenskikh, M.Chugunova, S.T.Fredrich-Thornton et al., *IEEE Trans. Nucl. Sci.*, **57**, 1211 (2010).
11. E.A.Vovk, T.G.Deineka, A.G.Doroshenko et al., *J. Superhard Mater.*, **31**, 252 (2009).
12. R.P.Yavetskiy, E.A.Vovk, A.G.Doroshenko et al., *Ceram. Int.*, **37**, 2477 (2011).
13. Yu.Zorenko, A.Voloshinovskii, V.Savchyn et al., *Phys. Status Solidi B*, **244**, 2180 (2007).
14. Yu.Zorenko, V.Gorbenko, E.Mihokova et al., *Radiat. Meas.*, **42**, 521 (2007).
15. A.Pujats, M.Springis, *Radiat. Eff. Defects Solids*, **155**, 65 (2001).
16. M.Puchalska, P.Bilski, *Radiat. Meas.*, **41**, 659 (2006).
17. S.B.Ubizskii, A.O.Matkovskii, N.Mironova-Ulmane et al., *Phys. Status Solidi A*, **177**, 349 (2000).

Люмінесцентні властивості нанозеренної кераміки та монокристалів $Y_3Al_5O_{12}$

Ю.Зоренко, Т.Возняк, В.Горбенко, А.Дорошенко, О.Толмачов, Р.Явецький, І.Петруша, В.Туркевич

Проведено порівняльні дослідження оптичного пропускання, термостимульованої люмінесценції та фотолюмінесценції з часовим розділенням при збудженні синхротронним випромінюванням в області фундаментального поглинання нанозеренної кераміки $Y_3Al_5O_{12}$ та монокристалів аналогічного складу. Властивості нанозеренної кераміки близькі до такої для монокристалів із значною концентрацією антивузельних дефектів Y_{Al}. Спостережені відмінності в оптичних та люмінесцентних властивостях кристалів та нанозеренної кераміки обумовлені більш високим ступенем дефектності нанозеренної кераміки, який виникає через нерівноважний характер її отримання та високу концентрацію міжзеренних границь.